Meeting future NO$_X$ emissions using an electric heater in an advanced aftertreatment system

Prathik Meruva[1], Andrew Matheaus[1]*, Christopher A. Sharp[1], James E. McCarthy Jr[2], Thomas A. Collins[3] and Ameya Joshi[3]

[1]Southwest Research Institute (SwRI), San Antonio, TX, United States, [2]Eaton (United States), Galesburg, MI, United States, [3]Corning Inc., Corning, NY, United States

Engine and aftertreatment solutions are being identified to meet the upcoming ultra-low NO$_x$ regulations on heavy duty vehicles as published by the California Air Resources Board (CARB) and proposed by the United States Environmental Protection Agency (US EPA) for the year 2027 and beyond. These standards will require changes to current conventional aftertreatment systems for dealing with low exhaust temperature scenarios. One approach to meeting this challenge is to supply additional heat from the engine; however, this comes with a fuel penalty which is not attractive and encourages other options. Another method is to supply external generated heat directly to the aftertreatment system. The following work focuses on the later approach by maintaining the production engine calibration and coupling this with an Electric Heater (EH) upstream of a Light-Off Selective Catalytic Reduction (LO-SCR) followed by a primary aftertreatment system containing a downstream Selective Catalytic Reduction (SCR). External heat is supplied to the aftertreatment system using an EH to reduce the Tailpipe (TP) NO$_x$ emissions with minimal fuel penalty. Two configurations have been implemented, the first is a Close Coupled (CC) LO-SCR configuration and the second is an Underfloor (UF) LO-SCR configuration. The CC LO-SCR configuration shows the best outcome as it is closer to the engine, helping it achieve the required temperature with lower EH power while the UF LO-SCR configurations addresses the real-world packaging options for the LO-SCR. This work shows that a 7 kW EH upstream of a LO-SCR, in the absence of heated Diesel Exhaust Fluid (DEF), followed by a primary aftertreatment system met the 2027 NO$_x$ regulatory limit. It also shows that the sub-6-inch diameter EH with negligible pressure drop can be easily packaged into the future aftertreatment system.

Introduction

The issues of global warming and ozone depletion urge a need to reduce our environmental emissions, and vehicle emissions are a major contributor to it, especially heavy-duty vehicles which constitute a significant portion of the on-road vehicles. The majority of the diesel vehicle emissions are comprised of oxides of nitrogen (NO_x), which are linked with several health and environmental risks. Historically, there have been several rounds of emission standards designed to reduce NO_x emissions from heavy duty on-road vehicles (Heavy-Duty Warranty Cost Study Report, 2019). The most aggressive recent standard is the Low NO_x Omnibus regulation adopted by the California Air Resources Board (CARB) to push the limits further, requiring a 90% reduction in NO_x from the current 0.20 g/hp-hr standard to 0.02 g/hp-hr starting model year (MY) 2027 while also meeting the existing requirements under Phase 2 Green House Gas (GHG) regulations to improve carbon dioxide (CO_2) (California Air Resources Board, 2019; California Air Resources Board, 2020).

There have been several advances to reduce NO_x emissions from heavy-duty engines (Milovanovic et al., 2016; Berndt, 2019; Zavala et al., 2020). The main area where the aftertreatment system struggles to reduce NO_x is during low exhaust temperature conditions, when the Selective Catalytic Reduction (SCR) catalytic activity is limited (Scott Sluder et al., 2005). Electric heaters are one of the technologies that has been investigated to provide additional heat required for the aftertreatment system to stay active and convert Engine Out (EO) NO_x emissions even during low exhaust temperatures.

There has been a significant work in the past to evaluate the need and performance of an Electric Heater (EH) towards reducing tailpipe (TP) NO_x. Given the concurrent need to minimize fuel consumption, it is important to manage any fuel penalty associated with the EH operation. Kasab et al. (Kasab et al., 2021a) found a fuel penalty of ~1% when adding an EH upstream of a close-coupled SCR. The resulting emissions were 0.018 g/hp-hr on Federal Test Procedure (FTP), meeting the 2027 CARB standards with a 10% margin. Webb et al. (Webb et al., 2021) measured emissions from a 2017 13L engine. The addition of a 48 V EH was found to be necessary to meet the Low Load Cycle (LLC) limit, but a significant fuel penalty of ~7% was recorded at 4 kW EH power.

Aftertreatment temperatures during a cold start has been improved by some recent work using a driven turbocharger with a turbine bypass to heat the aftertreatment system faster. Brin, J. (Brin et al., 2021) used the turbine bypass on a production engine with a mechanically driven turbocharger. This technology measured an increase in the aftertreatment temperature by 50°C or higher during the first 400 s of a cold FTP cycle with a reduced fuel consumption. It helps in achieving faster light off temperature for a SCR for better NO_x conversion and could be combined with the EH to get a better NO_x–CO_2 trade-off.

Similar combination of technology for a better NO_x–CO_2 trade-off is the use of Cylinder De-Activation (CDA) with the EH. Matheaus et al. (Matheaus et al., 2021) measured emissions from a 15 L engine modified to include CDA, and an advanced after-treatment including a 48 V EH upstream of an LO SCR with the maximum power of 5 kW. The use of an EH alone (without CDA) gave substantial NO_x reduction on a composite FTP however, it was accompanied with an undesired fuel penalty of ~1.5% vs. the CDA baseline. Additional work was performed on this experiment. Zavala et al. (Zavala et al., 2022) found that similar excellent NO_x control can be achieved with a maximum of 2.4 kW heating power. Reducing the heater power aids in reducing CO_2 since the engine is required to generate the electricity used to power the EH.

While this paper addresses electrical heat, testing with another heat source was performed on a similar non-CDA X15 with a more conventional setup (Harris et al., 2021; McCarthy et al., 2022). A fuel burner was placed upstream of the conventional AT system. Composite TP NO_x results for the FTP were 0.018 g/hp-hr with less than 1% increase in Brake Specific CO_2 ($BSCO_2$). TP NO_x results over the LLC was 0.006 g/hp-hr with a 9% increase in $BSCO_2$. A portion of the engine generated CO_2 was traded for the contribution of CO_2 by the burner.

Most of the ongoing research works to achieve 2027 NO_x regulations are with the addition of Light-Off Selective Catalytic Reduction (LO-SCR) to the current production aftertreatment systems (Kasab et al., 2021b; Sharp et al., 2021; Zavala et al., 2022). The LO-SCR gains a benefit of reaching the light off temperature faster than the primary SCR by staying closer to the engine. In practical applications, packaging of the LO-SCR near the engine compartment is a difficult task; however, this work has the LO-SCR positioned at 42 inches for the Close Coupled (CC) LO-SCR configuration (shown in Figures 1C, 2A) and 8 feet downstream of the turbocharger for the Underfloor (UF) LO-SCR configuration (shown in Figures 1D, 2B) which offers many packaging options. This work focuses on addressing the packaging issue by using UF LO-SCR to reach the 2027 CARB NO_x standards while showing the benefit of having an CC LO-SCR configuration. The program is focused on using an EH upstream of LO-SCR with a maximum power of 7 kW in combination with a production engine and aftertreatment system representative of 2022 production. The EH heaters are analyzed on different aftertreatment configurations and compared with the baseline aftertreatment system to analyze the NO_x–CO_2 trade off.

Experimental setup

Engine platform

The test engine used for this program was a production 2018 model year Cummins X15 engine with a 500 hp production
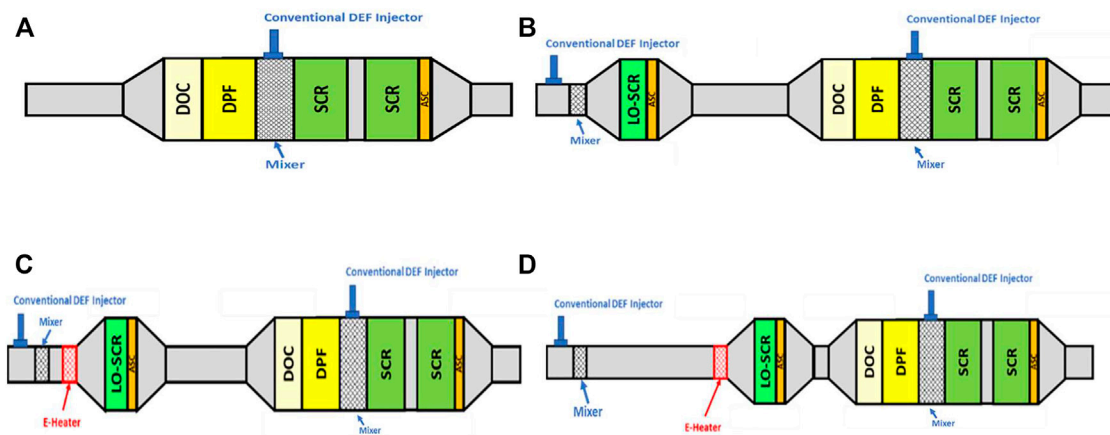
FIGURE 1
(A) Baseline 1 aftertreatment system schematic. **(B)** Baseline 2 aftertreatment system schematic with LO-SCR. **(C)** Aftertreatment system schematic with Close-Coupled (CC) LO-SCR and EH. **(D)** Aftertreatment system schematic with Underfloor (UF) LO-SCR and EH.
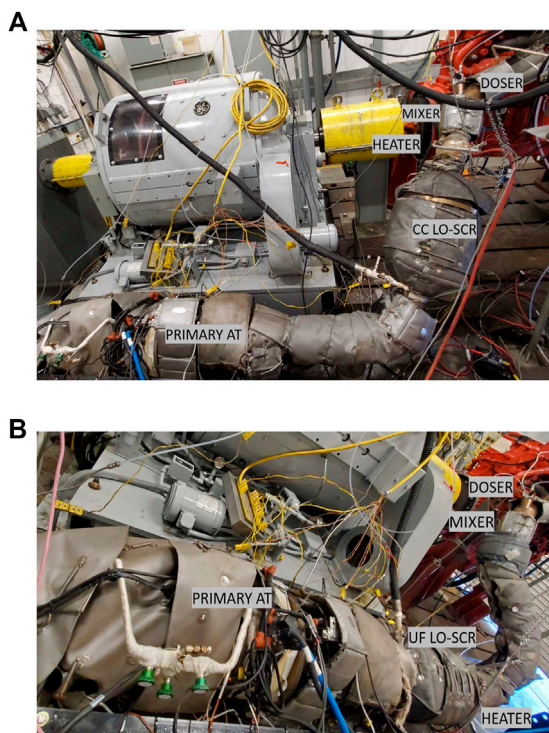
FIGURE 2
(A) Fully insulated aftertreatment system with CC LO-SCR and EH. **(B)** Fully insulated aftertreatment system with UF LO-SCR.

FIGURE 3
Cummins X15 engine platform installed in test cell.

calibration similar to the engine utilized in the CARB Stage 3 on-road baseline testing (Sharp et al., 2021). The engine retained the production air handling system, Exhaust Gas Recirculation (EGR) system, internal components, and fuel system. The engine is as shown in Figure 3. The baseline aftertreatment system was representative of the catalysts in production for the 2022 model year which will be discussed later.

Electric heater (EH)

During the 1990's, EH concepts were explored to improve the cold start emissions (Reddy et al., 1994; Weiss et al., 1995; Hampton et al., 1996). These heaters were based on thin discs of a high temperature steel honeycomb. The resistance of the

FIGURE 4
(A) Drawings of an electric catalyst heater (Anderson et al., 2021). Item 10 represents the heater disc, 22 and 24 the support rings, and 20 the insulation packaging material. **(B)** Image of the packaged heater.

heater disc was adjusted to a target value by adding slits (in the element) to extend the electrical path length. The packaging of the heater disc used support rings or analogous structures, resulting in a self-supporting design, requiring no further axial support. Examples from the original work are shown in Figure 4.
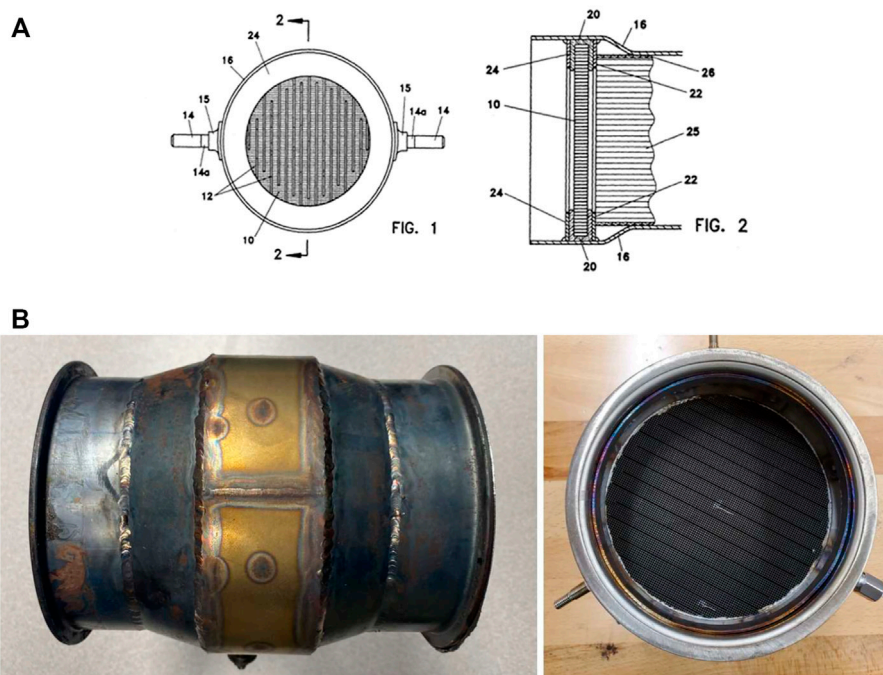
An electrical potential (voltage) is applied during the "get hot" mode to the two electrodes resulting in an increase in heater body temperature through Joule heating. The industry is considering moving over to 48 V systems to power electric heaters and other accessories. In this work, a 48 V system to power a 7 kW EH results in a reasonable current limit of 145 amps. Much of the work in this paper had a maximum power setting of 5 kW which drops the maximum current to 105 amps. This is a reasonable current level for the time in which the EH is turned on.

Heater discs have cell densities of 300–450 Cells Per Square Inch (CPSI), which provide an excellent ratio of surface area for heat transfer to the gas and are 5–10 mm thick. The high efficiency and compact design make these honeycomb-based heater components very attractive. The product design is very flexible and allows design of the heater to any resistance, within the practically relevant range (currently ca. 200–500 mOhm).

The details of the catalyst heater used in this study can be found in Table 1. It should be noted that while it is possible to put a catalyst on the heater, the heater was not catalyzed in this work,

TABLE 1 Catalyst heater specifications.

Parameter	Value
Element diameter	143.8 mm
Thickness	5.08 mm
Mass	173.5 g
CPSI	400
Web thickness	0.15 mm (6 mil)
Resistance	320 mOhm
Support ring ID	133.6 mm
Can length	51 mm

so it heats the gas stream transferring the heat to the downstream catalyst components *via* convection. The heater can be considered in its simplest and cheapest form.

The sample was packaged in the "Prototype" canning with the insulating material and support rings (Anderson et al., 2021), within a stand-alone can (no downstream catalyst directly attached), enabling placement within the exhaust pipe before the entrance cone to the LO-SCR. The setup had a bed thermocouple on the EH for monitoring purpose. The control algorithm utilized gas thermocouples for feedback temperature control which would be the intent for production applications.

TABLE 2 Baseline 1 system catalyst specifications.

Component	D × L	CPSI	Volume (L)
DOC	$13'' \times 5''$	400	11
DPF	$13'' \times 7''$	300	15
SCR	$13'' \times 6''$	600	13
SCR-ASC	$13'' \times 6''$	600	13

TABLE 3 Baseline 2 and EH testing catalyst specifications.

Component	D × L	CPSI	Volume (L)
LO-SCR	$13'' \times 6''$	400	13
DOC	$13'' \times 5''$	400	11
DPF	$13'' \times 7''$	300	15
SCR	$13'' \times 6''$	600	13
SCR-ASC	$13'' \times 6''$	600	13

Aftertreatment

The aftertreatment system has two distinct baselines. **Baseline 1** is a primary aftertreatment system consisting of Diesel Oxidation Catalyst (DOC), Diesel Particulate Filter (DPF), compact mixer, Selective Catalytic Reduction (SCR) and Ammonia Slip Catalyst (ASC) and is representative of a 2022 model year. This system has a conventional a Diesel Exhaust Fluid (DEF) injector mounted on the mixer. Schematic representation of this system is shown in Figure 1A. Table 2 shows the catalyst volumes for this 2022 production like aftertreatment system.

Baseline 2 is a system that builds on Baseline 1 by adding a LO-SCR and another conventional DEF injector. There have been many relative studies that show the merit of adding a LO-SCR for cold start operation as this is a smaller catalyst that can heat up quickly when positioned closed to the engine. An illustration of the Baseline 2 aftertreatment system is shown in Figure 1B. There is a mixer located after the DEF injector.

Previous work (Sharp et al., 2021) utilized a heated doser in front of the LO-SCR. A heated doser allows DEF dosing down to 130°C exhaust temperature instead of the normal dosing temperature of 180°C for most advanced SCR systems. This study utilized a conventional doser (non heated) in front of the LO-SCR. With conventional dosing, the temperature required to begin dosing is 180°C to ensure proper DEF vaporization and prevention of urea deposits. However, later in this work, with the use of an EH, the LO-SCR temperature rises very fast so the use of a heated doser is considered not necessary. The difference between 130 and 180°C during a cold FTP is approximately a 5 s delay in dosing DEF. For reference, the same temperature difference at the downstream primary SCR is an 84 s delay and occurs much later in the cycle due to the thermal masses involved. The catalysts specifications, for Baseline 2 and EH tests are listed in Table 3, which includes the addition of an upstream LO-SCR catalyst system.

This program focuses on utilizing a LO-SCR and external heat supply upstream of the LO-SCR system shown in Table 3 as depicted by Figure 1C. The EH was placed ahead of the LO-SCR to enable NO_x reduction as soon as possible. Heater control targeted the average gas temperature (inlet and outlet) of the LO-SCR.

There were two approaches to the LO-SCR aftertreatment configuration in this program that is relevant to packaging on a Class 8 Truck: 1) Close-Coupled (CC) LO-SCR and 2) Underfloor (UF) LO-SCR. The first approach was to represent a similar aftertreatment configuration as the Stage 3 Low NO_x program (Sharp et al., 2021) and the second approach was to consider a real-world issue of packaging the LO-SCR on the chassis rail. As mentioned earlier, Figure 1B shows the baseline configuration of the LO-SCR. This setup is referred to as close-coupled, because the LO-SCR is as close to the turbine outlet as possible. This was kept constant in this study while the configuration of EH and LO-SCR was allowed to vary from in the close coupled and underfloor configurations. However, the distances are representative of placing the LO-SCR directly under the passenger steps.

The electric heater was similar in size to exhaust system and was easily integrated into the system. The mixer was located between the DEF doser and the electric heater. The illustration of the heater location is shown in Figure 1C. A photograph of the setup is shown in Figure 2A.

Exhaust insulation will likely be required to meet 2027 emissions regulations. Current one-box systems already reduce exhaust cooling and provide insulation. The work in this paper utilized exhaust blankets to retain heat similar to the Stage 3 work (Sharp et al., 2021). Limiting the cooling of the exhaust system will help to reduce power consumption of the EH or energy consumption of other heating strategies and should be considered for serial production.

The UF LO-SCR scenario was accomplished by moving the LO-SCR further away from the engine and closer to the DOC of the primary downstream system. A photograph of the setup is shown in Figure 2B. The EH stayed positioned in front of the LO-SCR while the doser and mixer remained close to the turbine exit. Hence, the only aftertreatment system that was moved was the EH and LO-SCR. An illustration of the system is shown in Figure 1D. A true UF LO-SCR configuration would be approximately six feet. In the test cell, the distance was longer to fully capture the appropriate worst-case distance. Hence, eight feet, as tested, would be an extreme length of UF configuration.

Table 4 provides the distances between the engine turbo out, LO-SCR and DOC for the different aftertreatment configurations. Baseline 1, which included only the primary

TABLE 4 Change in length for UF aftertreatment.

Distances	CC LO-SCR (inches)	UF LO-SCR (inches)
Turbo-out to LO-SCR	42	96
Between LO-SCR and DOC	51	18
Turbo-out to DOC	93	132

AT system, was configured with 93 inches from the engine turbo out to the DOC. Baseline 2, which included the LO-SCR; configuration lengths are the same as the CC LO-SCR values.

The aftertreatment system used in this work was hydrothermally aged by utilizing an accelerated aging protocol on a burner based aging platform. The aging protocol targeted the aftertreatment system with the equivalent amount of thermal exposure for a Full Useful Life (FUL) system i.e., 435,000 miles or 9,800 h of service accumulation time similar to previous works (Matheaus et al., 2021; McCarthy et al., 2022; Zavala et al., 2022). The catalysts at the end of this aging cycle are commonly referred to as "Development Aged" end of life catalysts. The difference between "Developed Aged" and "Real World Exposed to Chemical Poisoning" is characterized in previous works (Sharp et al., 2021).

A model-based controller (Sharp et al., 2017; Rao et al., 2020; Sharp et al., 2021) was being used in this program to control the DEF dosing similar to the baseline work (Meruva et al., 2022) and also the thermal management strategies to power on the EH. The model tracks ammonia storage in each of the SCR substrates and has a target ammonia storage based on temperature. The DEF doser configurations were the same between the tests with the EH and their respective baseline tests (Meruva et al., 2022). The model-based control is discussed in Meruva, et al. (Meruva et al., 2022).

Electric heater (EH) power

The EH was powered up by an external power supply in the same way as previous work (Zavala et al., 2022) and similar to representative burner work (McCarthy et al., 2022). The control algorithm was Proportional Integral Derivative (PID) control as a basis and varied the voltage output of the power supply from 0 to 48 V. In this work, the feedback control for the PID was based on the average LO-SCR temperature. The average LO-SCR temperature was taken from the inlet and the outlet gas temperatures of the LO-SCR. These were production thermocouples that protrude 2 inches from the wall. This is consistent with other EH works in the past (Matheaus et al., 2021; Zavala et al., 2022). The voltage and current measurements were recorded at the EH and used to calculate the electrical power supplied to it. In real-time, a parasitic load was applied to the engine assuming an 80% generator efficiency. This is assuming a mild hybrid system with efficient power generation. Alternator

efficiencies are known to be lower than 80%. The engine was not given credit for this parasitic load in the cycle work. However, CO_2 and NO_x emissions due to this additional load were included in the analysis. The formula used for the real-time addition of load is show in Eq. 1.

$$Total\ Engine\ Torque\ (Nm) = Cycle\ Torque\ (Nm)$$
$$+ \frac{\frac{EH\ Power\ (KW)}{0.8} * 9548.8}{Engine\ Speed\ (rpm)} \quad (1)$$

Emissions measurements

Emission testing in this work were performed on a motoring/absorbing engine dynamometer test cell utilizing raw exhaust measurements complying with a Code of Federal Regulations Part 1065. The measurement equipment used included the following:

- A raw Horiba MEXA 7000 series each for the engine out and TP emissions sampling
- An FTIR for LO-SCR out NO_x emission measurements

The variability of NO_x measurement is ~ ± 0.001 g/hp-hr and CO_2 measurement is ~ ± 2 g/hp-hr. This is true for all the results discussed in this work.

Test cycles evaluated

Multiple key test cycles were evaluated using the engine and aftertreatments systems described above. These include the Heavy-Duty FTP and the LLC. Additional real world driving cycles evaluated were the Beverage Cycle and the Stay Hot Cycle. Finally, the European World Harmonized Transient Cycle (WHTC) was evaluated.

Federal test procedure (FTP)

United States Environmental Protection Agency (US EPA) and CARB use the US Heavy-Duty FTP standard regulatory drive cycle for evaluation of emission standards. The regulatory

FTP composite NO_x limit for 2027 has been set to 0.02 g/hp-hr. Composite results are calculated as 6/7 of hot FTP and 1/7 cold FTP. This is a well-known cycle, so it is not shown here.

Low load cycle (LLC)

The LLC is a composite of multiple real-world driving cycles. Data was collected over various applications and combined to form this cycle. A problem with the FTP as an evaluation cycle is that it has higher loads than many real-world situations. Due to the higher-than-normal loads, the exhaust temperatures are much hotter, and the SCR system stays active. The LLC cycle was developed to be more realistic of use and has been approved as a regulatory cycle. These lighter loads force the exhaust temperatures to be much lower and NO_x control becomes a challenge. The cycle is 5535 s in duration and is preceded by an FTP cycle with a 20-min soak period between them. The regulatory NO_x limit for LLC cycle for 2027 has been set to 0.05 g/hp-hr.

Beverage cycle

The Beverage cycle is a subset of the LLC and is derived from a service truck delivering Beverages or packages. This cycle has idle sections that are longer than 1 min and several transient ramps. The average load is 7.1%. Four Beverage cycles (800 s each) are connected to form a test. The initial two cycles were for thermal conditioning. The emission values were quantified for the final two cycles only. The authors have found the Beverage cycle to be an excellent cycle for controls optimization as is much shorter (~4 cycles in less than 1 h) than the LLC (~1.5 h) while the load factors are nearly identical.

Stay hot

The Stay Hot drive cycle involves conditioning the engine and the aftertreatment system at a preset speed and load till the temperatures attain steady state. This is succeeded by a 40-min idle period before returning to the previous load and speed conditions. This cycle focuses on how a long idle impacts the NO_x conversion efficiency of the aftertreatment system during the idle and immediately after a return to service.

World harmonized transient cycle (WHTC)

The WHTC drive cycle is based on the global pattern of real heavy-duty commercial vehicle usage. It is a transient engine dynamometer cycle. The United Nations Economic Commission for Europe, Working Party on Pollution and Energy group developed the Global Technical Regulation group which covers a worldwide harmonized heavy-duty certification procedure for engine exhaust emissions. Composite WHTC values are calculated by 14% cold and 86% hot. This is also a well-known cycle, so it is not shown here. Typically, a European engine would be tested for the WHTC while for this work, a US production engine was tested for this cycle. As such, these results give an indication of what may be possible while no effort was spent to truly represent a European engine calibration.

Results and discussion

The section shows the test results performance comparison of the CC LO-SCR and the UF LO-SCR configurations using different drive cycles which are FTP, LLC, Beverage, Stay Hot and the WHTC. These results demonstrate that using an EH with maximum power of 7 kW upstream of a LO-SCR in combination with a production engine and an aftertreatment system representative of 2022 production will be able to achieve NO_x standards for the MY 2027.

This project used two baseline aftertreatment systems. The baseline 1 was to represent the current 2022 production aftertreatment system while baseline 2 added the upstream LO-SCR to baseline 1 configuration. Baseline 2 is important for this work as the LO-SCR was used with all the EH results.

Baseline 1: Representative of 2022 aftertreatment system (without LO-SCR)

Baseline 1 (shown in Figure 1A) emissions are shown in Table 5. Please note that the SCR is larger than what would be in production for this engine and model year. Therefore, these emissions are better than what a 2018 engine + aftertreatment system would yield. The FTP composite Brake Specific NO_x ($BSNO_x$) value is 6.5 times higher than the limit of 0.02 g/hp-hr. For the LLC, the baseline 1 value is 18 times the limit of 0.05 g/hp-hr. Even with the larger aftertreatment system, additional technology is required to reduce NO_x emissions, primarily at lighter loads.

Baseline 2: Added LO-SCR to baseline 1

The baseline 2 (shown in Figure 1B) test results for both the above-mentioned configurations are the same as our previous works for a non-CDA engine with a conventional DEF doser (unheated DEF) for the LO-SCR (Meruva et al., 2022) and the summary of those results are as shown in Table 5. The composite FTP NO_x value is three times the limit. The LLC value is more

TABLE 5 Baseline 1 and Baseline 2 emission test results

Configuration		Baseline 1			Baseline 2			
Cycle	Units	BSNO$_x$		BSCO$_2$	BSNO$_x$			BSCO$_2$
		EO	TP		EO	LO-SCR out	TP	
Cold FTP	g/hp-hr	2.18	0.209	524.6	2.00	0.45	0.159	529.5
Hot FTP	g/hp-hr	2.70	0.116	503.1	2.77	0.71	0.043	504.9
Composite FTP	g/hp-hr	*2.60*	*0.129*	*506.2*	*2.66*	*0.67*	*0.060*	*508.5*
LLC	g/hp-hr	4.00	0.918	619.2	4.10	2.68	0.716	614.9
Beverage	g/hp-hr	4.08	2.147	698.2	4.06	3.60	1.669	686.3
Stay Hot	g/hp-hr	3.20	0.428	644.0	3.14	1.37	0.238	655.9
Cold WHTC	g/kW-hr	4.28	0.232	676.8	3.98	1.53	0.245	678.8
Hot WHTC	g/kW-hr	5.34	0.093	654.1	5.00	2.08	0.125	659.2
Composite WHTC	g/kW-hr	*5.19*	*0.112*	*657.3*	*4.86*	*2.01*	*0.142*	*661.9*

TABLE 6 FTP composite, cold FTP, and hot FTP test results

Cycle	Configuration	BSNO$_x$ (g/hp-hr)			BSCO$_2$ (g/hp-hr)	Integrated heater power consumption (kW-hr)
		EO	LO-SCR Out	TP		
Cold FTP	Baseline 1	2.18	—	0.209	524.6	—
	Baseline 2	2.00	0.45	0.159	529.5	—
	CC LO-SCR	1.98	0.31	0.075	542.5	0.67
	UF LO-SCR	2.10	0.29	0.095	546.6	0.79
Hot FTP	Baseline 1	2.70	—	0.116	506.2	—
	Baseline 2	2.77	0.71	0.043	504.9	—
	CC LO-SCR	2.69	0.44	0.010	512.7	0.40
	UF LO-SCR	3.20	0.41	0.012	512.4	0.48
Composite FTP	Baseline 1	2.60	—	0.129	506.2	—
	Baseline 2	2.66	0.67	0.060	508.5	—
	CC LO-SCR	2.59	0.42	0.019	517.0	—
	UF LO-SCR	3.04	0.40	0.024	517.3	—

than 14 times the limit. The baseline is also not within the EURO VI regulations of 0.46 g/kW-hr for the composite WHTC. Just adding a LO-SCR does not immediately remedy the high NO$_x$ values. Engine calibration/optimization would improve on these values. However, additional technologies are still required to meet 2027 emissions standards.

Composite FTP

Table 6 shows the FTP composite values of both the CC LO-SCR (shown in Figure 1C) and the UF LO-SCR (shown in Figure 1D) configurations, with the EH upstream of the LO-SCR, as these are compared to both baseline results. The CC

configuration is within the NO$_x$ regulatory limit of 0.02 g/hp-hr for the year 2027. The UF configuration exceeds the limit; however, the UF configuration was tested without any changes to the calibration and the authors believe that tuning the model will reduce the TP NO$_x$ values. This is still a significant finding as there is considerable additional distance and metal surface area. Both the EH configurations had a NO$_x$ conversion efficiency of over 99%. Observing the LO-SCR NO$_x$ out values, the LO-SCR reduced 75% of the EO NO$_x$ for Baseline 2. The LO-SCR reduced 84% of the EO NO$_x$ in the CC configuration. Finally, in the UF configuration, the LO-SCR reduced 87% of the EO NO$_x$. With this said, the LO-SCR is not specifically designed to handle all the engine out NO$_x$. There is room to optimize LO-SCR size.
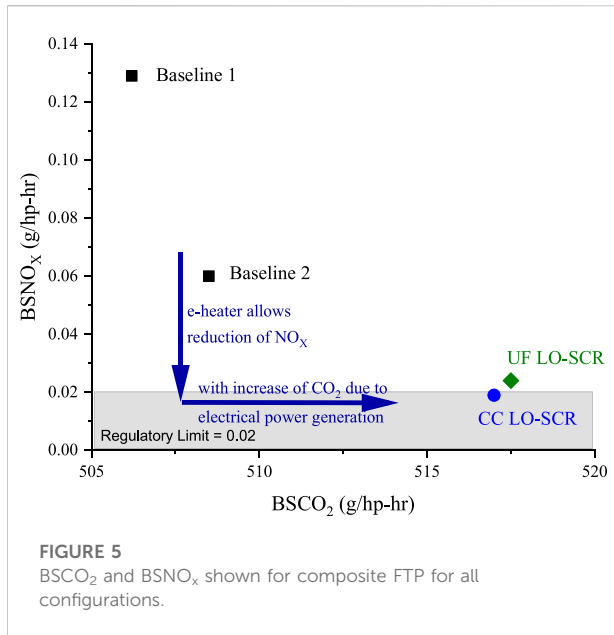
FIGURE 5
$BSCO_2$ and $BSNO_x$ shown for composite FTP for all configurations.

The composite results in Table 6 are shown graphically in Figure 5. As observed in Table 6, UF LO-SCR seems to slightly better NO_x conversion than the CC LO-SCR as the UF LO-SCR is closer to the downstream aftertreatment system which helps in preserving thermal inertia of the catalyst, which is lower in the case of a CC LO-SCR. The EH cases reduce TP NO_x significantly with a modest penalty in CO_2. The heater control strategy for FTP was the same between both the configurations with a maximum power consumption of 7 kW and the average LO-SCR target gas temperature of 235°C (average LO-SCR T = $(T_{in}+T_{out})$/2). The control temperature on the LO-SCR was 10°C higher than the optimal value found in (Zavala et al., 2022); however, it is good to see that the values are very close between 225 and 235°C.

Cold FTP

The cold FTP results are shown in Table 6. The CC configuration provided the lowest TP NO_x emissions with only 0.67 kW-hr of electrical energy used. The UF configuration required 0.79 kW-hr of energy and had higher TP NO_x emissions than the CC variant. Ideally, the cold FTP NO_x emissions target is 0.08 g/hp-hr to have enough margin for the composite calculation. Increasing the distance of the aftertreatment system from the engine inherently allows the exhaust to cool down further so increased heater power is expected. Also, the UF configuration may benefit from a different heater control logic to reduce TP NO_x.

Requiring the engine to generate the power for the EH shows up in higher CO_2 numbers. Naturally, the higher electrical

consumption yields higher CO_2. Less than 1 kW-hr of energy is required to reduce the cold TP NO_x emissions in the range to meet 2027 emissions limits. The energy is spent during the first 600 s of the FTP.

Figure 6 shows a graphical comparison of the CC LO-SCR and the UF LO-SCR configurations to Baseline 2 for the cold FTP cycle. The heater is required for the first half of the FTP because this is the lighter loaded portion. After 600 s, the engine generates enough heat to keep the SCR in an optimum temperature range.

Observing the LO-SCR average temperature, the EH does a great job of raising the exhaust temperature above 200°C by 105 s for the CC, and 138 s for the UF. A large portion of the NO_x emissions is emitted during the first acceleration (~45 s). This can be seen in the cumulative TP NO_x graph. Since the CC system reaches more optimum temperature faster, it can start reducing NO_x on the first acceleration. The UF does not reach temperature as quickly, so it matches Baseline 2 for the first acceleration. At the second accelerations (218 s), both CC and UF are reducing a large portion of the NO_x emissions. Baseline 2 is still below optimum temperature. By the third acceleration (382 s), both CC and UF configurations are effectively reducing NO_x.

At approximately 200 s, the heater control logic on the CC configuration starts to reduce power. This can be observed on the instantaneous heater power graph as it starts to pulse. For the UF configuration, the heater stays at maximum power for a longer period. The impact on electrical consumption is shown on the cumulative heater power graph.

Hot FTP

Table 6 shows the numerical comparison of both the configurations along with the baselines for the hot FTP cycle. There are some variations in EO NO_x due to test-to-test variation. The engine is expected to operate on two different modes; assumed as thermal management mode and fuel economy mode. The engine switches between these modes based on the aftertreatment temperature. In the case of the UF configuration, as the aftertreatment system temperature is slightly higher than other configurations the engine is expected to stay on fuel economy mode for a longer duration which is expected to be the cause of a higher EO NO_x. Both EH configurations reduce TP $BSNO_x$ to levels appropriate to meet 2027 emissions.

The EH $BSCO_2$ values are 1.4% higher than baseline values because the engine is required to generate the electricity consumed by the EH. This is not a fair comparison because if the baseline engine was calibrated in a manner to meet 2027 emissions standards, the $BSCO_2$ will likely be higher than reported here. One such technique, retarding injection
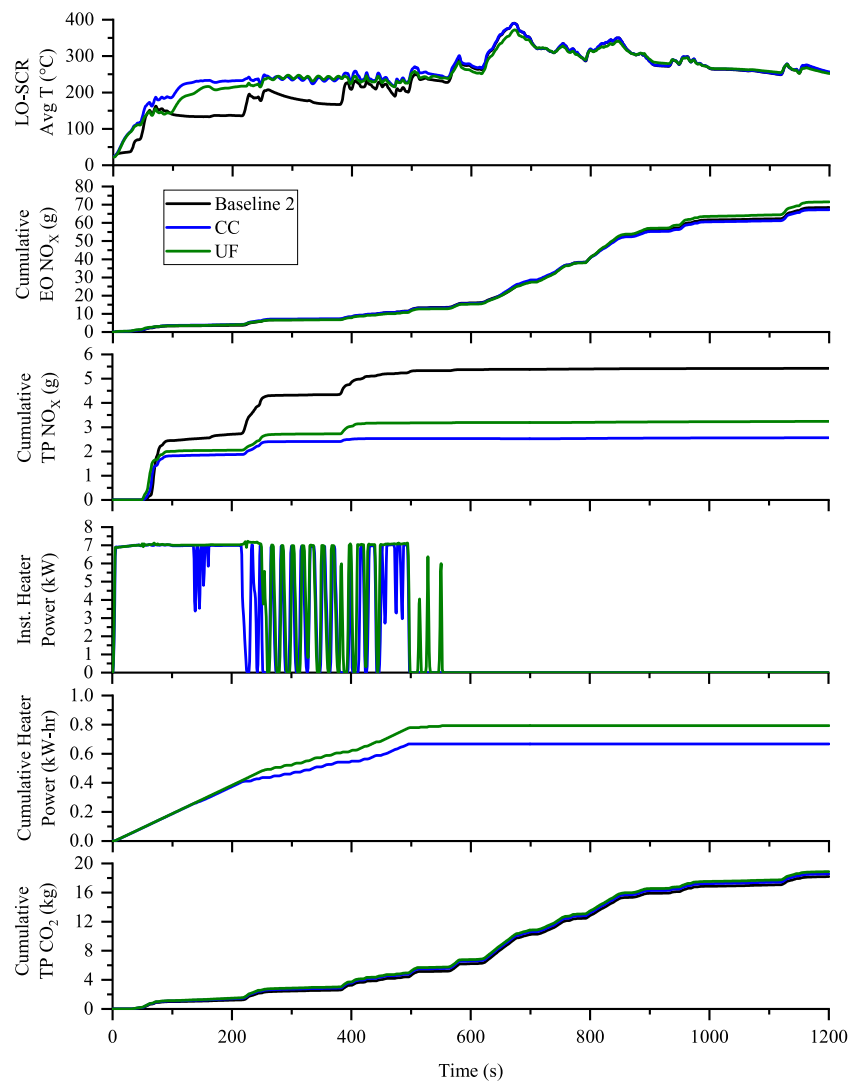
FIGURE 6
Comparison of the CC LO-SCR and UF LO-SCR to Baseline 2 on a Cold FTP cycle for the LO-SCR average temperature, emissions, and heater electrical power consumption.

timing, is known to increase fuel consumption and CO_2 emissions.

A graphical comparison of the CC and UF configurations to the baselines are shown in Figure 7. Since the hot FTP follows the cold FTP with a 20-min soak, there is enough thermal heat retained in the substrates that the NO_x generated in the first acceleration is reduced in all configurations. The LO-SCR substrate cools down during the idle portions of the FTP. This shows up as increased TP NO_x emission for the second and third accelerations on the cumulative TP NO_x graph. The EH configurations have NO_x fully under control by the third acceleration. The EH controller in both configurations start reducing power early in the cycle. The integrated electrical consumption is 0.40 and

0.48 kW-hr for the CC and UF, respectively. The hot FTP uses 40% less electrical power than the cold FTP, irrespective of the configuration.

Low load cycle (LLC)

Results for the LLC cycle are shown Table 7. The EO NO_x emissions are higher for the heater configurations indicating that the engine was operating in a more fuel-efficient mode. Aftertreatment temperatures are the primary basis for determining the mode of operation. The engine is allowed to operate more efficiently when the aftertreatment system is hot.
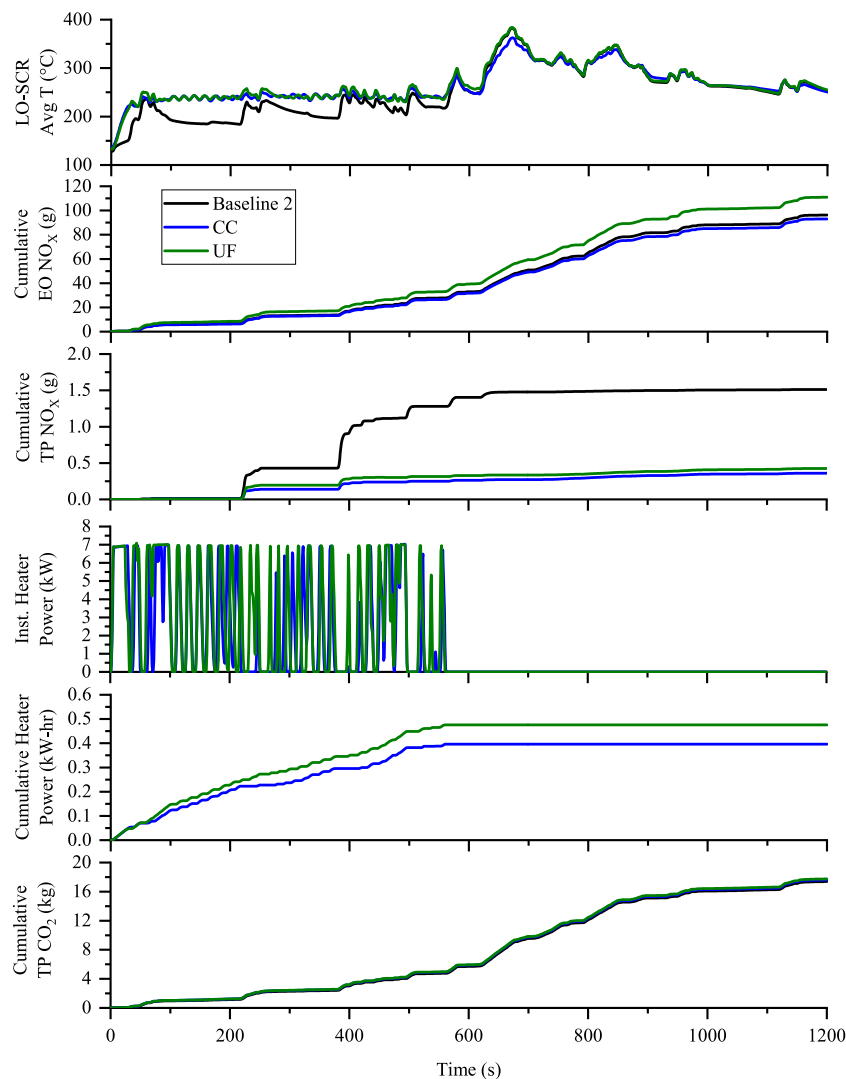
FIGURE 7
Comparison of the CC LO-SCR and UF LO-SCR to Baseline 2 on a Hot FTP cycle for the LO-SCR average temperature, emissions, and heater electrical power consumption.

The heater control strategy for the LLC cycle was set to target 225°C as the average LO-SCR temperature with 5 kW max heater power. Electrical energy consumption is much greater for the LLC than seen on the FTP tests. The LLC is 1.5 h long compared to the 20-min FTP. Overall lower loaded cycle with a longer test duration yields an increased electrical demand which directly increases CO_2. The UF configuration had a lower TP NO_x but a higher electrical energy consumption than the CC configuration.

The cycle results for the LLC are graphically shown in Figure 8. The NO_x regulatory limit for this cycle is 0.05 g/hp-hr. The dramatic reduction in $BSNO_x$ is apparent when utilizing the EH. Also apparent is the increase in $BSCO_2$. However, the baseline CO_2 numbers are at a much higher NO_x value. The

actual CO_2 numbers for a non-EH 2027 solution is not known at this time. It can be assumed that NO_x reduction comes at a cost of CO_2 unless a technology such as CDA is utilized.

The comparison graph for the LLC is provided in Figure 9. The LO-SCR average temperature for both EH cases is considerably higher than Baseline 2, which accounts for the excellent NO_x reduction (*see* cumulative TP NO_x graph). Both configurations had an increased average temperature of 52°C when compared to Baseline 2. Both configurations operated with the same heater strategy which was 5 kW maximum heater power and an average LO-SCR setpoint of 225°C. The UF configuration consumed 14% more power than the CC configuration, mostly on the first half of the cycle.

TABLE 7 LLC test results.

Configuration	BSNO$_x$ (g/hp-hr)			BSCO$_2$ (g/hp-hr)	Integrated heater power consumption (kW-hr)
	EO	LO-SCR out	TP		
Baseline 1	4.00	—	0.918	619.2	—
Baseline 2	4.10	2.68	0.716	614.9	—
CC LO-SCR	4.81	1.25	0.049	660.8	5.26
UF LO-SCR	4.77	0.88	0.014	656.5	5.99

FIGURE 8
Cycle results for the LLC.
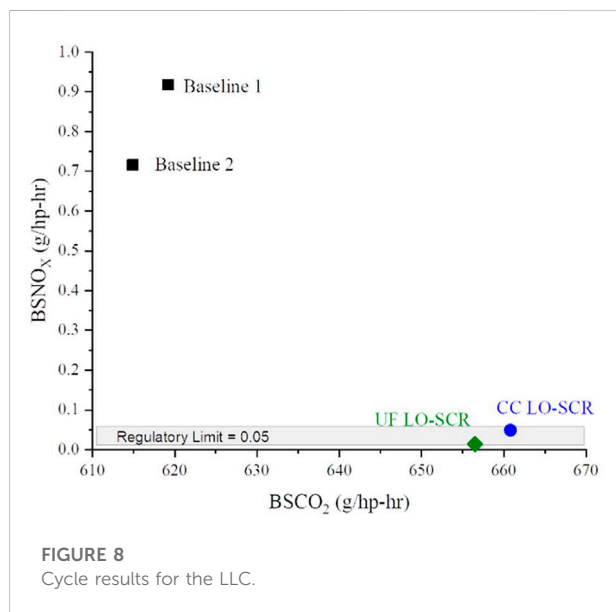
Beverage cycle

Table 8 shows the numerical comparison of both the configurations along with the baselines for the Beverage cycle. This is a good "in-use" evaluation of delivery trucks such as UPS, Coca-Cola, and Amazon. This is also a good representation of highly congested traffic areas such as Brazil. Both EH cases show over 99% NO$_x$ conversion efficiency with similar heater power consumption. On average, the EH cases had 11% higher CO$_2$ than the baseline cases.

Figure 10 shows the graphical comparison for the Beverage cycle. The heater control strategy was the same as the LLC cycle: 225°C average LO-SCR target with 5 kW max heater power. The average LO-SCR for Baseline 2 over the cycle was 163°C. This still allowed for a 59% NO$_x$ conversion efficiency due to ammonia storage. However, additional NO$_x$ control is required to meet emissions requirements. The EH in the CC configuration had an average temperature increase of 54°C. The EH in the UF configuration had an average temperature increase of 52°C.

The cumulative heater power values are nearly identical for the two cases, slightly over 2 kW-hr.

Stay hot

The Stay Hot test results are shown in Table 9. Both EH cases show a 99% NO$_x$ conversion efficiency. Similar TP NO$_x$ are achieved between the two cases with similar heater power consumed. These emissions are within the 2027 in use standards.

Multiple heater strategies were tested, and the best NO$_x$/CO$_2$ tradeoffs are presented in this paper. For the CC LO-SCR, the best strategy was a maximum heater power of 5 kW and a single setpoint of 225°C targeting the average LO-SCR temperature. The heater strategy for the UF LO-SCR configuration is different and is shown in Table 10. Since the UF configuration is much closer to the primary AT system, the most efficient strategy tried used the primary SCR inlet temperature as feedback. Since these are closer together, the EH also impacts the primary SCR temperature.

The multi-tier thought process is to minimize the electrical power needed. One way to minimize fuel consumption and CO$_2$ increase is to limit the maximum heater power. In some cases, however, the limited power does not allow for enough heat generation and there is NO$_x$ break through. The multi-tier strategy was developed so that when the target catalyst is colder, then a higher maximum electrical power and a higher setpoint temperature is allowed. As the target catalyst increases in temperature, the maximum power allowed and the setpoint temperature are reduced to minimize the electrical power consumption and thereby minimizing CO$_2$. The multi-tier approach was applied in different ways by targeting different catalyst temperatures.

The graphical comparison for the Stay Hot tests is provided in Figure 11. The EH for the CC case turns on 239 s after drop to idle. The EH turns on for the UF case at 388 s after drop to idle. For the UF case, the strategy is limiting maximum EH power due to the temperature of the primary SCR. At 1250 s, the primary SCR is cooling off and the maximum heater power is increased slowly over time. There is a difference in average LO-
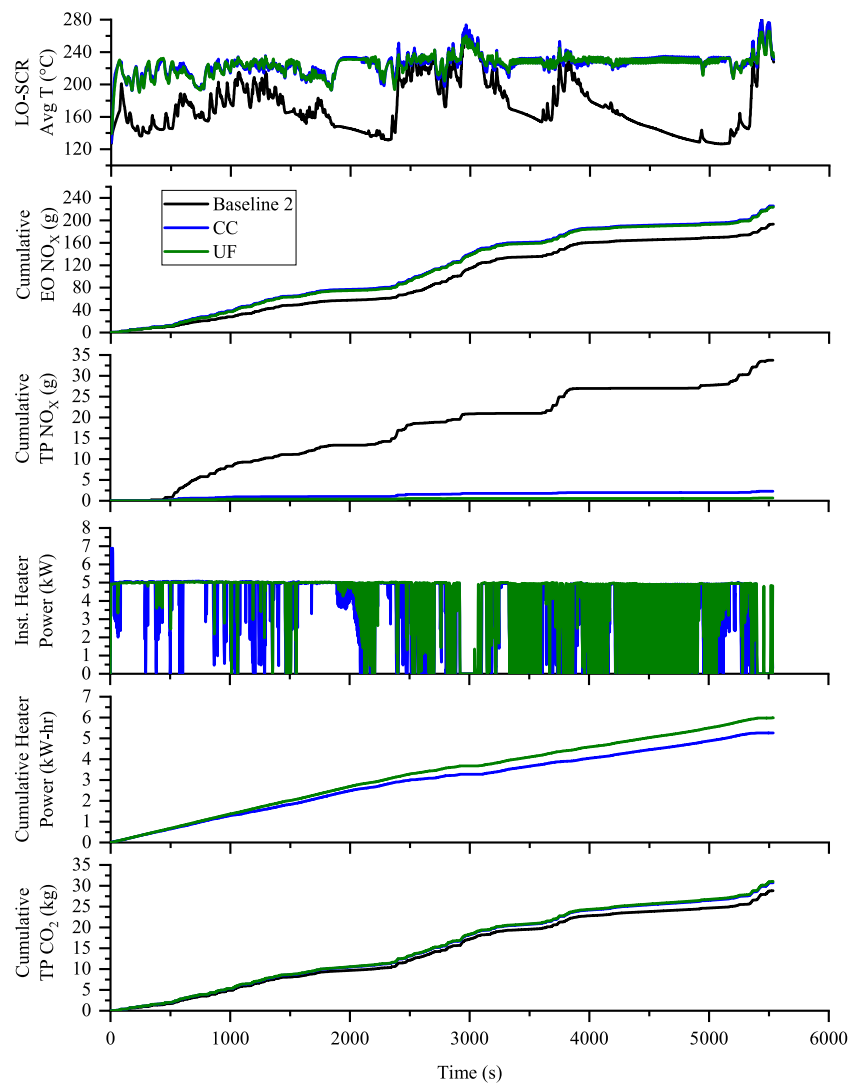
FIGURE 9
Comparison of the CC LO-SCR and UF LO-SCR to Baseline 2 on the LLC cycle for the LO-SCR average temperature, emissions, and heater electrical power consumption.

TABLE 8 Beverage cycle test results.

Configuration	BSNO$_x$ (g/hp-hr)			BSCO$_2$ (g/hp-hr)	Integrated heater power consumption (kW-hr)
	EO	LO-SCR out	TP		
Baseline 1	4.08	—	2.147	698.8	—
Baseline 2	4.06	3.60	1.669	686.3	—
CC LO-SCR	6.03	1.62	0.019	762.5	2.03
UF LO-SCR	5.89	1.67	0.033	775.6	2.15

Note that the in-use limits set by CARB in the low NO$_x$ rule are higher than the certification lab test cycle limits by a factor of 2 for model years 2024 through 2029. Accordingly, while the NO$_x$ limit on the HD-FTP cycle is 0.020 g/bhp-hr for MY 2027, the corresponding in-use limit is 0.040 g/bhp-hr (for intermediate life of 435,000 miles). It is seen that the above results on the Beverage cycle are within these in-use limits with 50% margin for the CC LO-SCR case.
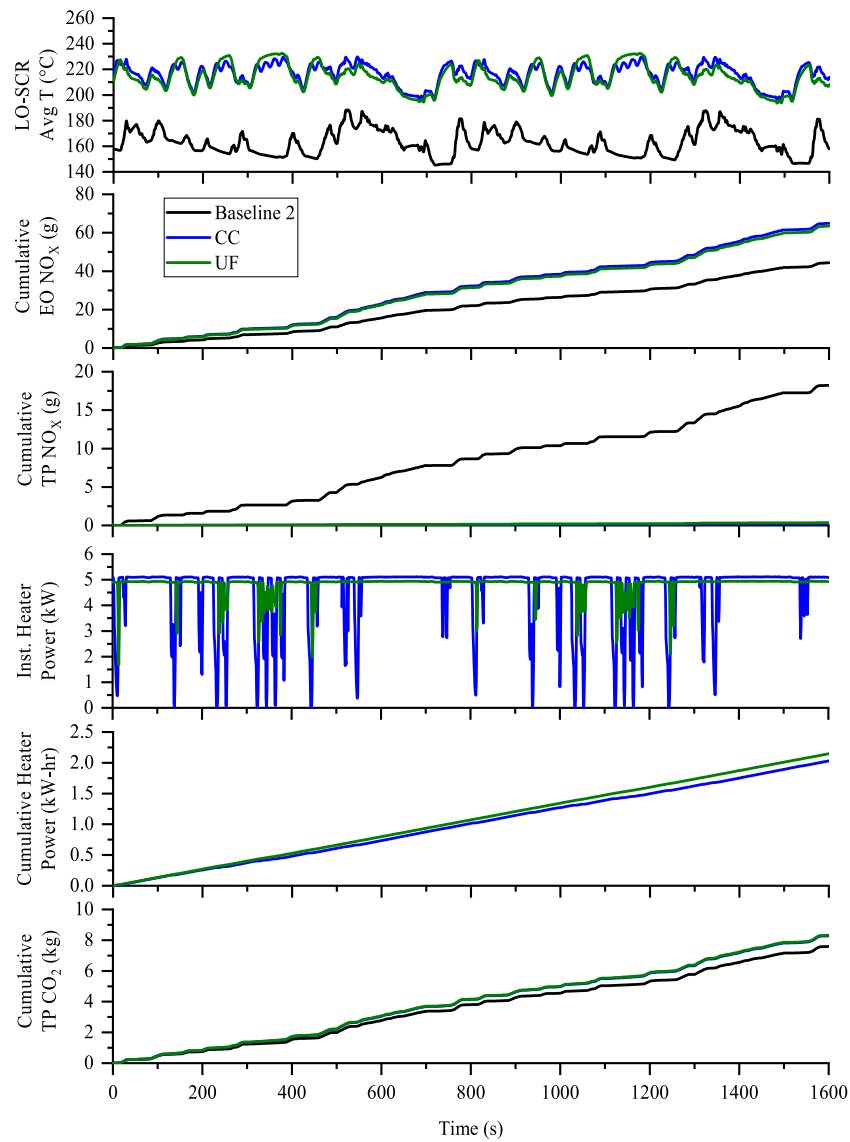
FIGURE 10
Comparison of the CC LO-SCR and UF LO-SCR to Baseline 2 on the Beverage cycle for the LO-SCR average temperature, emissions, and heater electrical power consumption.

TABLE 9 Stay Hot test results.

Configuration	BSNO$_x$ (g/hp-hr)			BSCO$_2$ (g/hp-hr)	Integrated heater power consumption (kW-hr)
	EO	LO-SCR out	TP		
Baseline 1	3.20	—	0.428	644.0	—
Baseline 2	3.14	1.37	0.238	655.9	—
CC LO-SCR	3.67	1.23	0.021	679.9	1.80
UF LO-SCR	3.93	0.29	0.016	687.8	1.51

TABLE 10 Multi-tier heater control strategy based on downstream SCR temperature.

Primary SCR Avg T (°C)	Max heater power (kW)	LO-SCR Avg setpoint T (°C)
0	7	235
150	7	235
190	5	220
200	3	210
≥210	2.4	200

FIGURE 11
Comparison of the CC LO-SCR and UF LO-SCR to Baseline 2 on the Stay Hot cycle for the LO-SCR average temperature, emissions, and heater electrical power consumption.
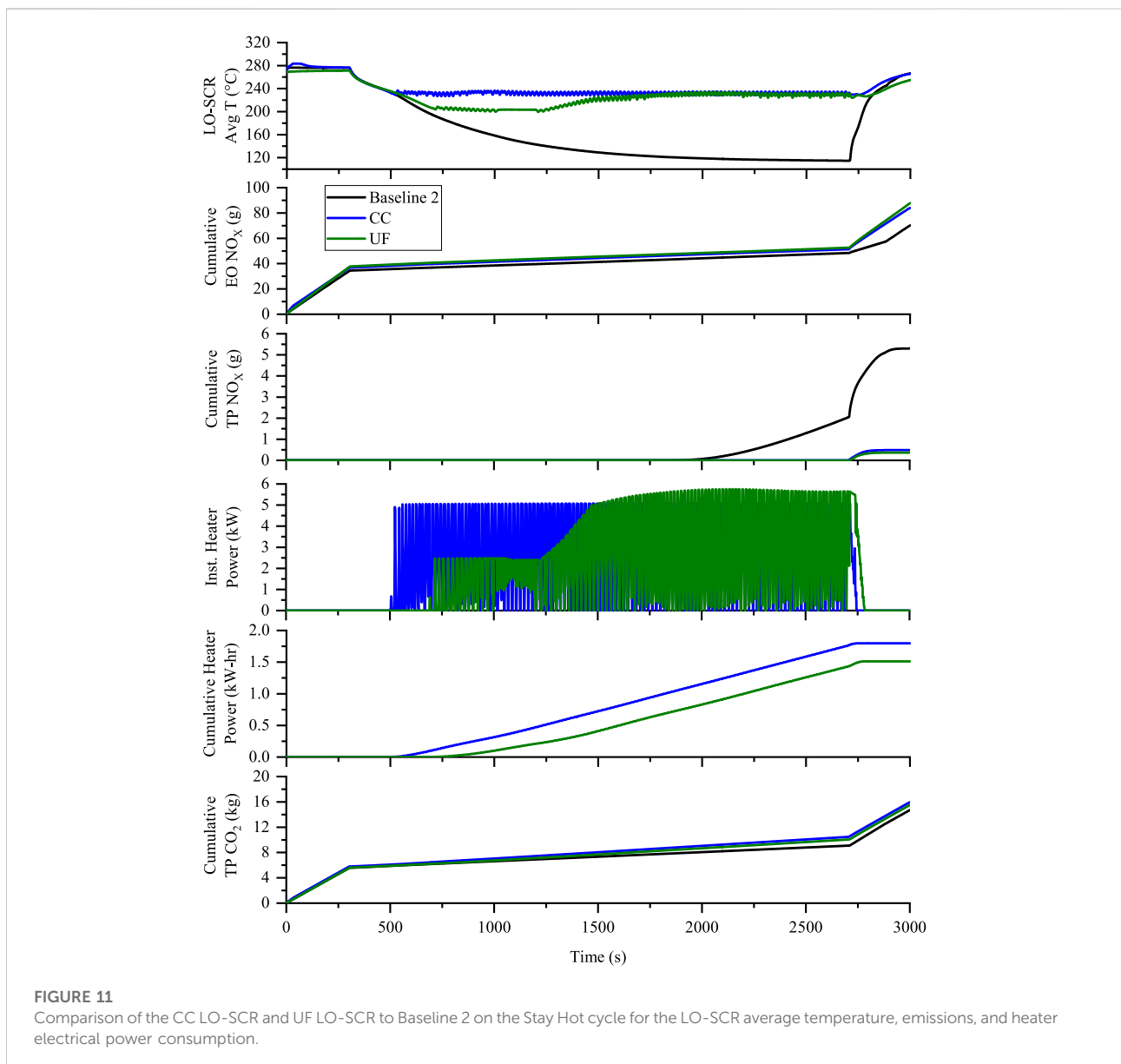
TABLE 11 Composite WHTC, cold WHTC and hot WHTC test results.

Cycle	Configuration	BSNO$_x$ (g/kW-hr)			BSCO$_2$ (g/kW-hr)	Integrated heater power consumption (kW-hr)
		EO	LO-SCR out	TP		
Cold WHTC	Baseline 1	4.28	—	0.232	676.8	—
	Baseline 2	3.98	1.53	0.245	678.8	—
	CC LO-SCR	4.20	1.35	0.095	692.4	0.88
	UF LO-SCR	4.41	0.56	0.145	691.3	1.19
Hot WHTC	Baseline 1	5.34	--	0.093	654.1	—
	Baseline 2	5.00	2.08	0.125	659.2	—
	CC LO-SCR	6.10	2.15	0.031	666.1	0.66
	UF LO-SCR	5.85	0.90	0.007	661.1	0.87
Composite WHTC	Baseline 1	5.19	--	0.112	657.3	—
	Baseline 2	4.86	2.01	0.142	661.9	—
	CC LO-SCR	5.83	2.04	0.040	669.8	—
	UF LO-SCR	5.65	0.86	0.026	665.3	

FIGURE 12
Comparison of the CC LO-SCR and UF LO-SCR to Baseline 2 on the cold WHTC for the LO-SCR average temperature, emissions, and heater electrical power consumption.
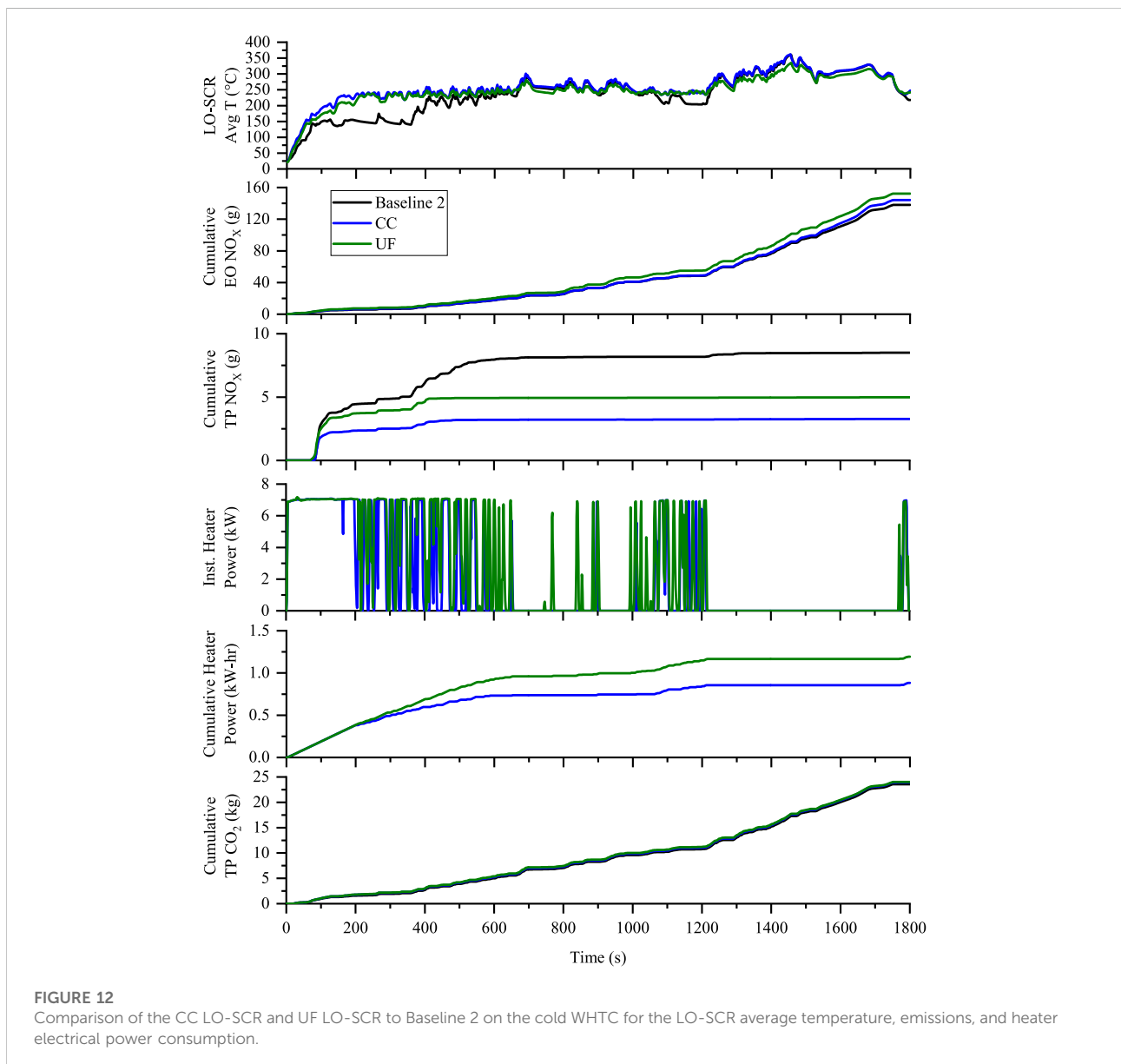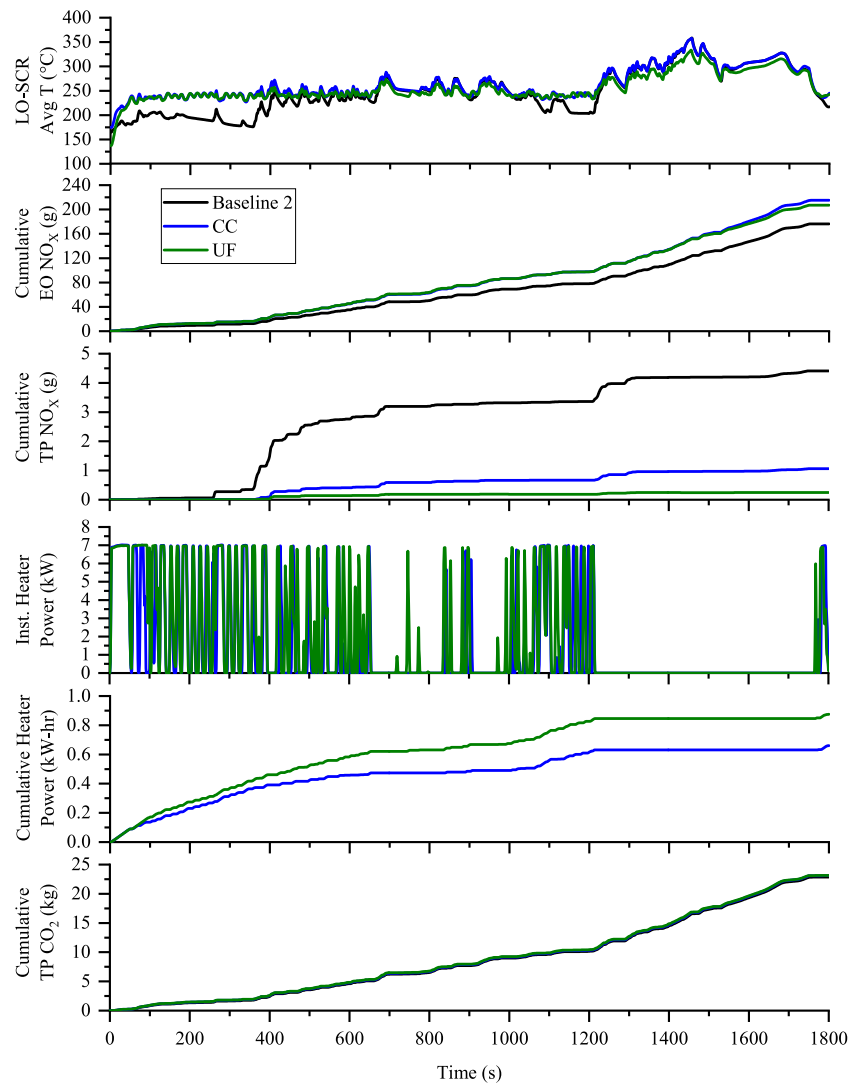
FIGURE 13
Comparison of the CC LO-SCR and UF LO-SCR to Baseline 2 on the hot WHTC for the LO-SCR average temperature, emissions, and heater electrical power consumption.

SCR temperature during the maximum power limited period (800–1250 s). Afterward, the average LO-SCR temperatures converge. The benefit of the multi-tier strategy shows up as a reduced cumulative integrated power. Observing the cumulative TP NO_x graph, Baseline 2 starts to have NO_x breakthrough at 2000 s. As the engine returns to service, there is a spike in TP NO_x. Both EH cases keep the NO_x breakthrough at a minimum.

Composite WHTC

The composite WHTC results are shown in Table 11. The baseline cases show a 97% NO_x reduction. The WHTC is a high

enough loaded cycle that the baseline configurations do well. The EH cases have over 99% NO_x reduction. The increase in $BSCO_2$ is minimal because the electrical power required is small. The EH control algorithm for all WHTC cases were targeting the LO-SCR average temperature to be 235°C and allowing the full 7 kW heater power, if needed.

Cold WHTC

The cold WHTC results are shown in Table 11. The NO_x conversion efficiencies for the baseline cases are in the low 90% range. The EH allows for higher NO_x conversion efficiencies (97%). The increase in CO_2 is 2% on average.

TABLE 12 Summary TP BSNO$_x$ and TP BSCO$_2$ test results.

Cycle	Units	TP BSNOx				TP BSCO2			
		Base 1	Base 2	CC	UF	Base 1	Base 2	CC	UF
Cold FTP	g/hp-hr	0.209	0.159	0.075	0.095	524.6	529.5	542.5	546.6
Hot FTP	g/hp-hr	0.116	0.043	0.010	0.012	503.1	504.9	512.7	512.4
Composite FTP	g/hp-hr	0.129	0.060	0.019	0.024	506.2	508.5	517.0	517.3
LLC	g/hp-hr	0.918	0.716	0.049	0.014	619.2	614.9	660.8	656.5
Beverage	g/hp-hr	2.147	1.669	0.019	0.033	698.2	686.3	762.5	775.6
Stay Hot	g/hp-hr	0.428	0.238	0.021	0.016	644.0	655.9	679.9	687.8
Cold WHTC	*g/kW-hr*	*0.232*	*0.245*	*0.095*	*0.145*	*676.8*	*678.8*	*692.4*	*691.3*
Hot WHTC	*g/kW-hr*	*0.093*	*0.125*	*0.031*	*0.007*	*654.1*	*659.2*	*666.1*	*661.1*
Composite WHTC	*g/kW-hr*	*0.112*	*0.142*	*0.040*	*0.026*	*657.3*	*661.9*	*669.8*	*665.3*

The graphical comparison for the cold WHTC is provided in Figure 12. The idle periods for the WHTC are roughly 200–360 s, 710–775 s, and 1150–1200 s. The EH is on from the start of the cycle to 650 s and from 1000 to 1200 s. It is not utilized much in other areas of the cycle. For the EH cases, most of the TP NO$_x$ is generated in the first 100 s.

Hot WHTC

The hot WHTC results are shown in Table 11. The hot test uses 25% less electrical energy than the cold test. The EH cases cut TP NO$_x$ by more than 60% when compared to baseline. The results are shown graphically in Figure 13. The EH controller maintains the average LO-SCR at or above 235°C. For the EH cases, the cumulative TP NO$_x$ is under 1 g. As before, the UF configuration used more electrical energy than the CC configuration.

Summary/conclusion

The test results from this program show that the CARB proposed 0.02g/hp-hr NO$_x$ target for the year 2027 can be achieved with a current production engine without any modifications to it. The following conclusions can be made from the above test data:

- A small EH coupled with a LO-SCR and downstream primary aftertreatment system can reduce the TP NO$_x$ emissions and reach an FTP composite of 0.02 g/hp-hr while also maintaining the NO$_x$ emissions within 0.05 g/hp-hr for an LLC cycle. A composite FTP NO$_x$ of

0.019 g/hp-hr was achieved with hydrothermal end-of-life aged catalysts. Using the same catalysts, TP NO$_x$ of 0.049 g/hp-hr for the close coupled configuration and 0.014 g/hp-hr NO$_x$ for the underfloor configuration was achieved for the LLC. The CC LO-SCR has an added benefit of being close to the engine which yields higher temperature for the catalyst helping in reducing the heater power required to be generated to keep the aftertreatment at the required temperature

- Considering that there are packing difficulties for the CC LO-SCR, even the UF LO-SCR that is positioned further downstream can help in achieving the 2027 NO$_x$ emissions with a minimal additional fuel penalty

A summary of all TP NO$_x$ and CO$_2$ results is shown in Table 12 that includes the FTP, LLC, Beverage, Stay Hot and WHTC with the LO-SCR in both the close coupled (CC) and underfloor (UF) configurations. The test data results prove that an EH with a maximum power capacity of 7 kW should a good viable option in reducing the NO$_x$ emissions and its maximum power capacity might be required only on few tests, especially during the cold starts but most of the hot cycles might just need a maximum power capacity of 5 kW.

Future work

CDA technology seems to be a viable option to increase the fuel economy and improve the aftertreatment thermal management as observed in previous works (Joshi et al., 2017; McCarthy, 2017; Ramesh et al., 2018; McCarthy, 2019). Future work could include adding CDA technology to the engine in combination with the EH technology to provide a better NO$_x$ vs. CO$_2$ trade off. This future

work is planned as a follow-up to previous work (Matheaus et al., 2021) using a smaller diameter EH in front of the LO-SCR while removing the heated DEF injector in front of the LO-SCR. The authors believe that adding the EH in this location will allow a standard, unheated DEF doser, to be used.

Data availability statement

The original contributions presented in the study are included in the article/Supplementary Material, further inquiries can be directed to the corresponding author.

Author contributions

All authors participated in developing the test plan and the outline of the paper. JM wrote abstract, introduction, and summary. TC and AJ wrote section about the EH. PM and AM conducted the testing and wrote about the test results, including the analysis. All authors participated in editing the final draft and adding additional information to tell the story.

Conflict of interest

Author JM was employed by Eaton (United States). Authors TC and AJ were employed by Corning Inc.

The remaining authors declare that the research was conducted in the absence of any commercial or financial relationships that could be construed as a potential conflict of interest.

Publisher's note

All claims expressed in this article are solely those of the authors and do not necessarily represent those of their affiliated organizations, or those of the publisher, the editors and the reviewers. Any product that may be evaluated in this article, or claim that may be made by its manufacturer, is not guaranteed or endorsed by the publisher.

References

Anderson, J. G., Collins, T. A., and Hampton, L. E. (2021). *Axially assembled enclosure for electrical fluid heater having a peripheral compression ring producing a diametrically balanced force*. Alexandria, VA: US patent office.

Berndt, C. (2019). *An experimental study of A passive nox adsorber (pna) for the reduction of cold start diesel emissions*. Houghton, Michigan: Michigan Technological University. Open Access Master's Thesis.

Brin, J., Keim, J., Christensen, E., and Holman, R. (2021). Applying a driven turbocharger with turbine bypass to improve aftertreatment warm-up and diesel nitrous oxides conversion. *SAE Int. J. Commer. Veh.* 14 (3), 391–407. doi:10.4271/02-14-03-0032

California Air Resources Board (2020). California adopts strong new regulation to further reduce smog-forming pollution from heavy-duty diesel trucks. Available at: https://ww2.arb.ca.gov/news/californiaadopts-strong-new-regulation-further-reduce-smog-formingpollution-heavy-duty.

California Air Resources Board (2019). Greenhouse gas standards for medium- and heavy-duty engines and vehicles. Available at: https://ww2.arb.ca.gov/our-work/programs/ghg-std-md-hd-eng-veh/about.

Hampton, L. E., Buhrmaster, C. L., and Thompson, D. F. (1996). *Durability of advanced electrically heated catalyst design*. United States: SAE International. doi:10.4271/960345

Harris, T., McCarthy, J., Jr., Sharp, C., Zavala, B., and Matheaus, A. (2021). *Meeting future NOx emissions limits with improved total fuel efficiency*. Rostock, Germany: Heavy-Duty, On- and Off-Highway Engines.

Heavy-Duty Warranty Cost Study Report (2019). California air Resources board staff current assessment of the technical feasibility of lower NOX standards and associated test procedures for 2022 and subsequent model year medium-duty and heavy-duty diesel engines. Available at: https://ww3.arb.ca.gov/msprog/hdlownox/white_paper_04182019a.pdf.

Joshi, M. C., Gosala, D. B., Allen, C. M., Vos, K., Van Voorhis, M., Taylor, A., et al. (2017). Reducing diesel engine drive cycle fuel consumption through use of cylinder deactivation to maintain aftertreatment component temperature during idle and low load operating conditions. *Front. Mech. Eng.* 8, 1. doi:10.3389/fmech.2017.00008

Kasab, J., de Monte, M., Hadl, K., Noll, H., Mannsberger, S., Graf, G., et al. (2021). Using close-coupled SCR to meet ultra-low NOx requirements. Available at: https://cleers.org/wp-content/uploads/formidable/3/2019CLEERS_Kasab_Web.pdf.

Kasab, J. J., Hadl, K., Raser, B., Sacher, T., and Graf, G. (2021). *Close-coupled SCR - an approach to meet ultra-low NOx requirements for heavy-duty diesel engines*. Ann Arbor, Michigan: CLEERS Virtual Workshop.

Matheaus, A., Neely, G., Sharp, C., Hopkins, J., and McCarthy, J. E., Jr (2021). Fast diesel aftertreatment heat-up using CDA and an electrical heater. *SAE Technical Paper 2021-01-0211*. doi:10.4271/2021-01-0211

McCarthy, J. E., Jr. (2019). *Simultaneous CO2 and NOX reduction for medium & heavy-duty diesel engines using cylinder deactivation*. Brazil: Sao Paulo.

McCarthy, J., Jr. (2017). *Cylinder deactivation improves diesel aftertreatment and fuel economy for commercial vehicles*. Stuttgart, Germany: 17th Stuttgart International Symposium.

McCarthy, J., Jr., Matheaus, A., Zavala, B., and Sharp, C. (2022). *Meeting future NO_X emissions over various cycles using a fuel burner and conventional aftertreatment system*. Detroit, Michigan: SAE Technical Paper 2022-01-0539. doi:10.4271/2022-01-0539

Meruva, P., Matheaus, A., Zavala, B., Sharp, C., and McCarthy, J. (2022). *Model based controller for advanced aftertreatment*. SAE International Journal of Commercial Vehicles.

Milovanovic, N., Hamalian, S., Lewander, M., and Larson, K. (2016). *The novel SCR and PNA exhaust gas after treatment systems for diesel passenger cars*. Springer. doi:10.1007/978-3-658-13255-2_4

Ramesh, A. K., Gosala, D. B., Allen, C. M., Joshi, M. C., Shaver, G. M., McCarthy, J., Jr., et al. (2018). *Cylinder deactivation for increased engine efficiency and aftertreatment thermal management in diesel engines*. United States: SAE International.

Rao, S., Sarlashkar, J., Rengarajan, S., Sharp, C., and Neely, G. (2020). A Controls Overview on Achieving Ultra-Low NOx. SAE Technical Paper 2020-01-1404. doi:10.4271/2020-01-1404

Reddy, K. P., Gulati, S. T., and LambertWeiss, D. (1994). *High temperature durability of electrically heated extruded metal support*. SAE Technical Paper 940782.

Scott Sluder, C., Storey, J., Lewis, S., and Lewis, L. (2005). *Low temperature urea decomposition and SCR performance*. SAE Technical Paper 2005-01-1858. doi:10.4271/2005-01-1858

Sharp, C., Neely, G., Zavala, B., and Rao, S. (2021). CARB low NO$_X$ stage 3 program-final results and summary. *SAE Int. J. Adv. & Curr. Prac. in Mobility* 3 (4), 1508–1525. doi:10.4271/2021-01-0589

Sharp, C., Webb, C., Neely, G., Sarlashkar, J., Rengarajan, S. B., Yoon, S., et al. (2017). Achieving ultra low NO$_X$ emissions levels with a 2017 heavy-duty on-highway TC diesel engine and an advanced technology emissions system - NO$_X$ management strategies. *SAE Int. J. Engines* 10 (4), 1736–1748. doi:10.4271/2017-01-0958

Webb, C., Stephenson, P., Meijer, M., and Coumans, A. (2021). *Future regulatory technology options to reduce risk in application for heavy-duty diesel engines*. Aachen, Germany: Aachen Colloquium Sustainable Mobility.

Weiss, D. S., Buhrmaster, C. L., Hampton, L. E., Powell, W., and Socha, L. S. (1995). Durability of extruded electrically heated catalysts. SAE Technical Paper 950404. doi:10.4271/950404

Zavala, B., McCarthy, J., Matheaus, A., and Sharp, C. (2022). *Fast diesel aftertreatment heat-up using CDA and an electrical heater between 1.2 and 5.0 kW*. Frontiers in Mechanical Engineering.

Zavala, B., Sharp, C., Neely, G., and Rao, S. (2020). *CARB low NOX stage 3 program - aftertreatment evaluation and down selection*. SAE Technical Paper 2020-01-1402. doi:10.4271/2020-01-1402